

Carbon, nitrogen, oxygen and lithium abundances of six cool supergiants in the SMC^{*}

V. Hill¹, B. Barbuy², and M. Spite¹

¹ Observatoire de Paris, Section de Meudon, DASGAL, URA 335 du CNRS, F-92195 Meudon Cedex, France

² Universidade de São Paulo, IAG, Dept. de Astronomia, CP 9638, São Paulo 01065-970, Brazil

Received 2 October 1996 / Accepted 2 January 1997

Abstract. Carbon, nitrogen and oxygen abundances were derived from high-resolution spectra of 6 cool supergiants of the Small Magellanic Cloud.

Oxygen-to-iron ratios (mean value $[\text{O}/\text{Fe}] \approx -0.18$ dex) are found to be similar to those found in young objects in the LMC and the Galaxy. This result is discussed in terms of chemical evolution. A mean deficiency of the carbon-to-iron ratio of $[\text{C}/\text{Fe}] \approx -0.3$ dex and a nitrogen-to-iron ratio $[\text{N}/\text{Fe}] \approx +0.22$ dex might imply a mixing signature, which is confirmed by the low $^{12}\text{C}/^{13}\text{C}$ ratio measured in three stars. In terms of chemical evolution, carbon plus nitrogen abundances have to be considered: in our sample, a mean value of $[(\text{C} + \text{N})/\text{Fe}] \approx -0.15$ dex indicates a slight deficiency in carbon plus nitrogen with respect to the Sun, similar to the deficiencies found in Galactic supergiants and Orion. Lithium has been detected in all the program stars, reaching $\epsilon(\text{Li})=0.6$ dex for two stars.

Key words: stars: abundances; supergiants – galaxies: abundances; evolution – Magellanic Clouds

1. Introduction

The star formation and therefore the chemical history of the Magellanic Clouds are different from that which occurred in the Galaxy. Detailed abundance determinations for different objects is essential to constrain efficiently the chemical evolution models. With the present day equipment, only the brightest youngest populations can be observed at high resolution, namely, supergiant stars, H II regions, Planetary Nebulae (PN) and Supernovae Remnants (SNR).

The CNO elements are key-elements for a better understanding of nucleosynthesis history. Oxygen is a reliable tracer of Supernovae Type II (SN II), carbon plus nitrogen abundances

reflect rather the enrichment by asymptotic giant branch winds, whereas carbon deficiencies and nitrogen enhancements indicate internal convective mixing effects in the stars. In the SMC, the carbon abundance has raised much interest since Dufour's (Dufour et al. 1982; Dufour 1984) very low carbon abundance determination for the H II regions, and the work by Rocca-Volmerange et al. (1981) showing that the extinction curve does not show the 2200 Å bump generally attributed to graphite grains.

Concerning the stars in the field of the SMC, the C, N, O elements are available only for a dozen objects (cf. Table 4), among which F supergiants (Luck & Lambert 1992, hereafter LL92; Russell & Bessell 1989, hereafter RB89; Spite et al. 1989a, hereafter SBS89) and B stars (Rolleston et al. 1993).

In the present work, we derive C, N and O abundances for a sample of six field cool (K) supergiant stars from high resolution échelle spectra. The basic stellar parameters for this sample, effective temperature (T_{eff}), surface gravity ($\log g$), metallicity ($[\text{Fe}/\text{H}]$) and microturbulent velocity (v_t) were taken from Hill et al. (1996, hereafter Paper I).

In Sect. 2 we describe the observations. The stellar parameters for the sample stars are presented in Sect. 3. CNO abundances are derived in Sect. 4. Concluding remarks are given in Sect. 5.

2. Observations and reductions

The sample stars were selected from the catalogue of Prévot et al. (1983) according to their ($B - V$) colours and visual magnitudes, in order to have a sample as homogeneous in temperature as possible; on the other hand, they were chosen to be widely spread out over the Small Magellanic Cloud in order to be able to check the homogeneity of the chemical composition of stars in various regions of the Cloud.

The observations were carried out at the European Southern Observatory (ESO) at La Silla, Chile using the New Technology Telescope (NTT) equipped with the ESO Multi-Mode Imager EMMI and the 3.6m telescope with the CASPEC spectrograph.

Send offprint requests to: V. Hill

* Based on observations collected at the European Southern Observatory, La Silla, Chile.

A resolution of $R = \lambda/\Delta\lambda \approx 20\,000$ and $28\,000$ for CASPEC and EMMI respectively were obtained.

The reductions were carried out using the code by Spite (1990). Further details on the data and a log-book of the observations are given in Paper I.

As in Paper I, the well studied galactic supergiant Arcturus was used as a reference. A spectrum of Arcturus with a slightly higher resolution and an excellent signal to noise ratio was kindly provided by M. Bessell.

3. Stellar parameters of the sample supergiants

The model atmospheres used in the analysis were computed by B. Plez (private communication) - see Plez et al. (1992) for a description of their model calculations. The grid consists of models for $5 M_{\odot}$ stars in the range of temperatures $3600 < T_{\text{eff}} < 4750$, in steps of 200/250 K, gravities $-0.5 < \log g < 3.5$ in steps of 0.5 dex, metallicities $-0.6 < [\text{Fe}/\text{H}] < +0.6$ in steps of 0.3 dex, and microturbulent velocity $v_t = 2 \text{ km s}^{-1}$. A code for interpolation in this grid was used to obtain the models corresponding to the stellar parameters of the sample stars.

In Table 1 are reported the instrument used, visual magnitude and given in Prévot et al. (1983), and the stellar parameters effective temperature T_{eff} , gravity $\log g$, metallicity $[\text{Fe}/\text{H}]$ and microturbulent velocity v_t obtained in Paper I.

In the derivation of stellar parameters, models with $\log g$ providing the ionisation equilibrium hypothesis have been adopted, although in these extended atmospheres, departures from LTE cause an overionisation effect. The gravity derived from stellar evolutionary tracks is higher by about 0.3 to 0.5 dex relative to the spectroscopic value where ionisation equilibrium is imposed, and the difference between the two gravity values corresponds to what is expected from the overionisation due to NLTE effects. A more detailed discussion on the stellar parameters derivation, in particular on gravity, is given in Paper I.

4. CNO abundances

Spectrum synthesis calculations were carried out to derive the carbon, nitrogen and oxygen abundances. A description of the spectrum synthesis code is given in Cayrel et al. (1991) and details on the molecular data in the wavelength range treated here are given in Milone et al. (1992). The code consists of a version improved along the years of the original code for atomic lines by Spite (1967) complemented for molecular lines by Barbuy (1981).

As in Paper I, the well studied galactic supergiant Arcturus (with a temperature very similar to the program stars) was used to check the quality of the physical data of the lines used in the abundance determination. The effective parameters used for Arcturus were: $(T_{\text{eff}}, \log g, [\text{Fe}/\text{H}]) = (4300, 1.5, -0.51)$ and $v_t = 1.7 \text{ km s}^{-1}$. The C, N and O abundances found for Arcturus are displayed in Table 2.

Moreover, in all the investigated regions, we checked the oscillator strengths of the atomic lines *nearby* the molecular

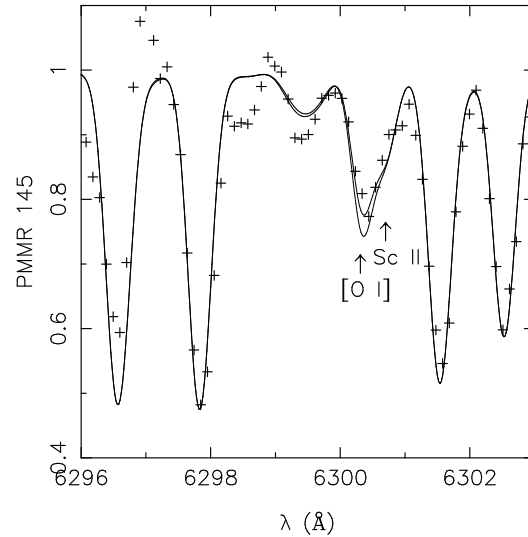


Fig. 1. $[\text{O I}]6300.3\text{\AA}$ in PMMR 145: Observed spectrum (crosses) and synthetic spectra computed with $[\text{C}/\text{Fe}] = -0.3$, $[\text{N}/\text{Fe}] = 0.1$, $[\text{O}/\text{Fe}] = 0.0$ and -0.1 (solid lines) ($[\text{Sc}/\text{Fe}] = -0.25$ was adopted from the detailed analysis).

features studied by fitting the Arcturus spectrum (using the elemental abundances found for Arcturus in Paper I).

Concerning the observed spectra, thanks to the overlapping between the orders, two independent spectra were available for most of the studied spectral regions. All spectra were checked and the best S/N spectrum was used.

4.1. Oxygen

Oxygen abundances were derived using the forbidden $[\text{O I}]\lambda 6300.311 \text{ \AA}$ line. The oscillator strengths used for the oxygen line and the ScII line nearby are those given in SBS89, whereas the Sc abundance has been determined from other lines (Paper I).

The oxygen abundance was then derived by fitting the observed $[\text{O I}]$ line with the line computed with different oxygen abundance values; let us note that the $[\text{O I}]$ and the nearby ScII lines form roughly in the same atmospheric layers (Lambert et al. 1974; Barbuy 1988) and that these lines are both very little affected by overionisation.

The final abundances were obtained iteratively, by taking into account the carbon and nitrogen abundances (Sec. 4.2 and 4.3) found for each star. For the star PMMR 27, since we could not derive the carbon abundance (due to the lack of observed spectrum in the corresponding wavelength domain) we adopted $[\text{C}/\text{Fe}] = -0.3$ in the calculations of dissociative equilibrium, similar to the underabundance found for the other stars (Sect. 4.2). This carbon deficiency, in turn, leads to a decrease of the oxygen abundance by about 0.1 dex relative to the solar carbon-to-iron case.

The resulting oxygen abundances are given in Table 2 and the fit for PMMR 145 is shown in Fig. 1.

Table 1. Stellar parameters adopted from Paper I

Star	Instrument	V	T _{eff}	log g	[Fe/H]	v_t (kms ⁻¹)
PMMR 23	EMMI	12.42	4200	0.2	-0.72	4.0
PMMR 27	EMMI	13.2	4300	0.0	-0.67	3.0
PMMR 48	EMMI	12.7	4300	0.3	-0.62	3.5
PMMR 102	EMMI/CASPEC	12.87	4300	-0.2	-0.70	3.5
PMMR 144	EMMI/CASPEC	12.82	4100	-0.7	-0.86	3.5
PMMR 145	EMMI	13.09	4300	0.3	-0.58	3.0
Arcturus			4300	1.5	-0.51	1.7

Table 2. CNO abundances

Star	[C/Fe]	[N/Fe]	[O/Fe]	[(C+N)/Fe]	C/N	C/O	C^{12}/C^{13}	$\epsilon(C)$	$\epsilon(N)$	$\epsilon(O)$	$\epsilon(Li)$
PMMR 23	-0.2	0.4	-0.10	-0.01	0.95	0.38	-	7.63	7.65	8.05	0.10
PMMR 27	-	0.1(:)	-0.20	-0.18	-	-	10	-	7.47	8.07	0.60
PMMR 48	-0.3	0.3	-0.10	-0.09	0.95	0.30	20	7.63	7.65	8.15	0.05
PMMR 102	-0.3	0.2	-0.30	-0.14	1.20	0.48	-	7.55	7.47	7.87	<0.00
PMMR 144	-0.4	0.2	-0.30	-0.19	0.95	0.38	-	7.29	7.31	7.71	0.10
PMMR 145	-0.3	0.1	-0.10	-0.18	1.51	0.30	20	7.67	7.49	8.19	0.55
Arcturus	0.	0.1	+0.30	0.02	3.02	0.24	7.2	8.04	7.56	8.66	<-0.30
Sun	0.0	0.0	0.00	0.0	3.80	0.48	89	8.55	7.97	8.87	1.16

(a) the standard notation $\epsilon(X) = \log N(X) = \log [n(X)/n(H)] + 12$, where n = number density of atoms is adopted; (b) the solar abundances adopted are from Grevesse & Noels (1993); (c) (:) the N abundance is dependent upon an unknown carbon abundance

4.2. Carbon

The $C_2(0,0)5165.24\text{\AA}$ and $C_2(0,1)5635.50\text{\AA}$ bandheads of the Swan ($A^3\Pi_g - X^3\Pi_u$) system were used to derive the carbon abundances. The $C_2(0,1)$ feature is weak in all the stars for which it is available. The $C_2(0,0)$ feature is stronger and, although blended with atomic lines and MgH, is more reliable. The values tabulated in Table 2 are thus the ones derived from the $C_2(0,0)$ feature. In most stars, this feature gives lower abundances (by 0.1 dex), and in two stars, both determinations agree.

The carbon abundances, available for five sample stars are given in Table 2.

For three of our most recent spectra, the region at 8003\AA was available, enabling us to distinguish the ^{12}CN from the ^{13}CN features. Fig. 2 displays the CN features in PMMR 27, computed with $[C/Fe] = -0.3$, $[N/Fe] = +0.1$ dex and a $^{12}\text{C}/^{13}\text{C}$ ratio of 10 and 29. For this star, the signal to noise ratio is high and the uncertainty on the ratio is estimated to be of around ± 5 . For the other two stars, the uncertainty is higher, around ± 10 .

4.3. Nitrogen

Nitrogen abundances were derived from the CN red system ($A^2\Pi - X^2\Sigma$) bandhead (6,2) $\lambda 6478.48\text{\AA}$. A check of several CN lines in the Arcturus spectrum indicated that this is essentially the only reliable CN feature in the wavelength region available.

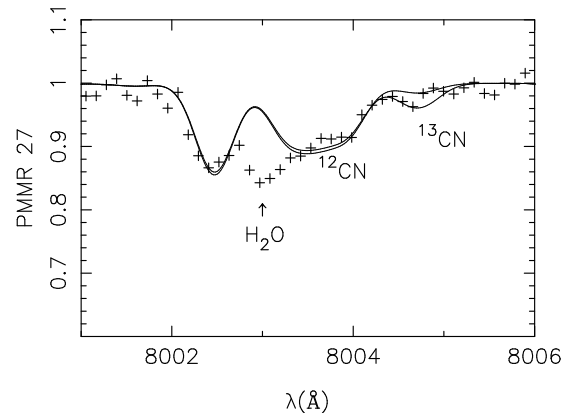


Fig. 2. PMMR 27: ^{12}CN and ^{13}CN features computed with $([C/Fe], [N/Fe]) = (-0.3, 0.1)$ and a $^{12}\text{C}/^{13}\text{C}$ ratio of 10 and 29 (solid lines) plotted against the observed spectrum (crosses).

For the nearby atomic lines, the abundances derived in Paper I were adopted.

For PMMR 27 for which the carbon abundance was not available, $[C/Fe] = -0.3$ was adopted. However, as we show in Fig. 3, the resulting CN feature is strongly dependent upon the carbon abundance; this figure displays the CN feature computed with $[N/Fe] = 0.1$ and $[C/Fe] = -0.1$ and -0.3 , and shows that

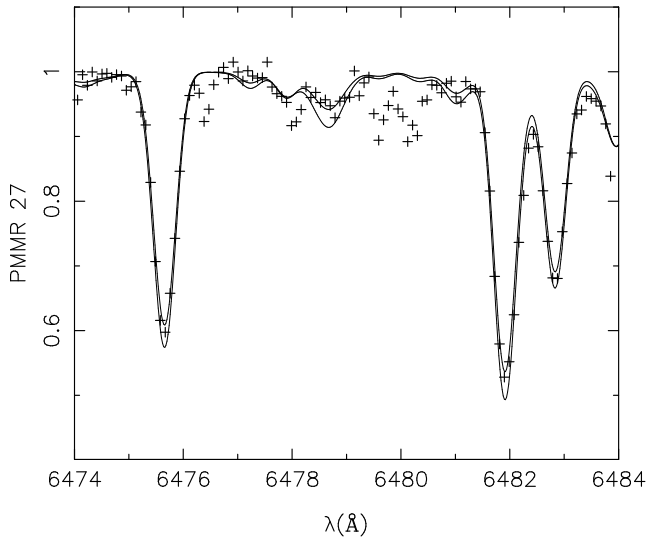


Fig. 3. PMMR 27: CN(6,2) feature computed with $[C/Fe]$, $[N/Fe] = (-0.3, 0.1)$ (adopted value) and $(-0.1, 0.1)$ (solid lines) plotted against the observed spectrum (crosses), illustrating the drastic dependence of the CN feature upon the carbon abundance.

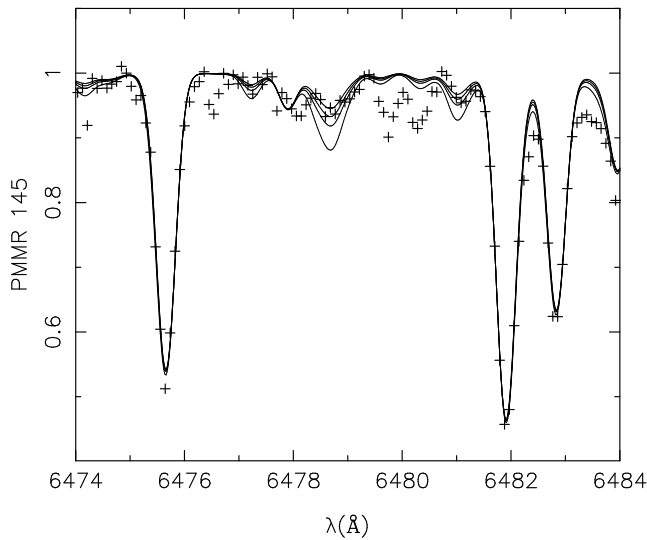


Fig. 4. CN(6,2) in PMMR 145: Observed spectrum (crosses) and synthetic spectra computed with $[C/Fe] = -0.3$ and $[N/Fe] = 0.0, 0.1, 0.2$ and 0.4 (solid lines).

a $\Delta[C/Fe] = -0.2$, leads to a $\Delta[N/Fe] = +0.25$. In Fig. 4 the CN feature in PMMR 145 is shown for $[C/Fe] = -0.3$ and $[N/Fe] = 0.0, 0.1, 0.2, 0.4$.

4.4. Lithium

The lithium abundance was derived from the 6707.8\AA line, taking into account the nearby atomic lines (and gf values) following Lambert et al. (1993) and the CN features. The oscillator strengths of the two ionised atomic lines Sm II, and

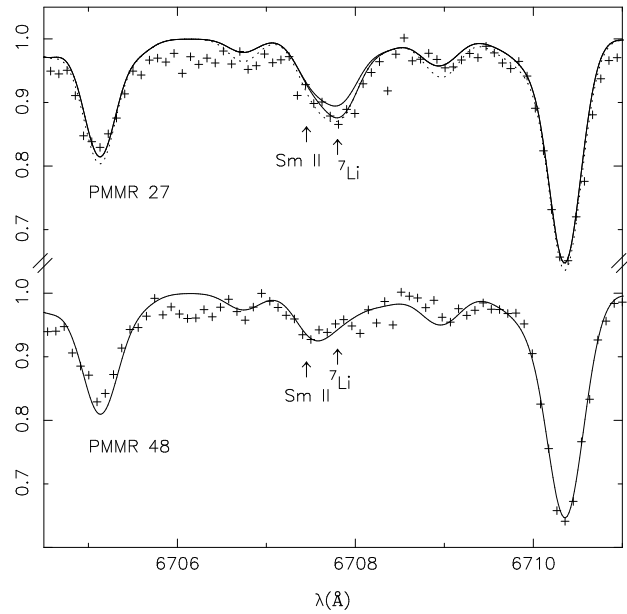


Fig. 5. Lithium line at 6707.8\AA in the "lithium-rich" star and a "lithium-poor" star: in PMMR 27: observed spectrum (crosses) and spectra computed with $[C/Fe] = -0.3$, $[N/Fe] = 0.1$ and $\epsilon(\text{Li}) = 0.60$ and 0.50 (solid lines); the dotted line is a spectrum computed with $[C/Fe] = -0.3$, $[N/Fe] = 0.1$ and $\epsilon(\text{Li}) = 0.60$ to show the location of the CN features in this region. in PMMR 48: observed spectrum (crosses) and spectra computed with $[C/Fe] = -0.3$, $[N/Fe] = 0.3$ and $\epsilon(\text{Li}) = 0.0$.

particularly important in these low gravity stars, were checked on the Arcturus spectrum and the gf of the Sm II line was fitted with $\log(gf) = -1.54$ dex (instead of -1.04 advised by Lambert et al. 1993). Fig. 5 shows two stars of our sample (with the same temperature): the richest and the poorest in lithium. For PMMR 27, we show two lithium abundance values (0.5 and 0.6 dex), as well as (in dotted line) the variation of the CN features upon a change of $+0.2$ dex in carbon abundance.

5. Discussion

In Table 3, we have gathered the C, N, O and iron abundance from all the available high resolution analyses in the Magellanic Clouds, for F supergiants (LL92, RB89, Spite et al. (1989b) and SBS89, Spite et al. 1993, Hill et al. 1995), B stars (Rolleston et al. 1993), together with the mean abundance for the Supernovae Remnants (Russell and Dopita 1990) and for the H II regions (Dufour 1984; Garnett et al. 1995). It should be noted that the more recent abundance determination of the Clouds' H II regions performed by Russell and Dopita (1990) gave results within 0.1 dex relative to the Dufour (1984) review. Moreover, from HST observations, Garnett et al. (1995) also found values of C and O compatible with Dufour. The values for Canopus (Luck & Lambert 1985) and B stars in Orion (Cunha & Lambert 1994) are also reported as Galactic references. We have corrected the abundances (relative to the Sun) in this table, to the presently accepted solar value from Grevesse et al. (1996).

Table 3. CNO abundances derived in supergiants from high resolution work available in the literature, and for reference objects (H II regions, supernovae remnants, Sun, Canopus and Orion)

Star	Source	[Fe/H]	[C/Fe]	[N/Fe]	[O/Fe]	$\epsilon(\text{C})$	$\epsilon(\text{N})$	$\epsilon(\text{O})$	$\epsilon(\text{C+N})$	$[(\text{C+N})/\text{Fe}]$	C/N	$\log(\text{C/O})$
SMC :												
F supergiants												
AzV121	1	-0.73	0.03	0.76	-	7.85	8.00	-	8.23	0.31	0.71	-
AzV369	1, 3	-0.51	-0.01	0.79	-0.11	8.03	8.25	8.25	8.45	0.31	0.60	-0.22
AzV140	3	-0.69	-0.11	-	-0.17	7.75	-	8.01	-	-	-	-0.26
AzV197	3	-0.51	-0.34	-	-0.20	7.70	-	8.16	-	-	-	-0.46
AzV127	2	-0.61	-0.34	-	-	7.60	-	-	-	-	-	-
AzV198	2	-0.75	-0.28	-	-	7.52	-	-	-	-	-	-
Mean (6 stars)	-	-0.63	-0.17	+0.77	-0.16	7.74	8.12	8.14	8.34	0.31	0.65	-0.31
std. dev.	-	± 0.11	± 0.17	-	± 0.04	± 0.18	-	± 0.12	-	-	-	± 0.13
B stars												
AzV304	4	-	-	-	-	7.75	6.87	8.47	7.80	-	7.59	-0.72
NGC346-11	4	-	-	-	-	7.75	7.47	8.27	7.93	-	1.91	-0.52
NGC346-737	4	-	-	-	-	7.65	7.07	8.17	7.75	-	3.80	-0.52
IDK-D2	4	-	-	-	-	7.35	6.67	-	7.43	-	4.79	-
LMC :												
F-G supergiants												
G244	5	-0.20	0.04	-	-0.17	8.39	-	8.50	-	-	-	-0.11
G258	5	-0.14	-0.19	-	-0.16	8.22	-	8.57	-	-	-	-0.35
G274	5	-0.34	-0.33	-	-0.06	7.88	-	8.47	-	-	-	-0.59
G319	5	-0.30	-0.17	-	-0.07	8.08	-	8.50	-	-	-	-0.42
G396	5	-0.30	-0.22	-	-0.02	8.03	-	8.55	-	-	-	-0.52
G406	5	-0.28	-0.22	-	-0.19	8.05	-	8.40	-	-	-	-0.35
G439	5	-0.24	-0.39	-	-0.28	7.92	-	8.35	-	-	-	-0.43
G501	5	-0.31	-0.07	-	-0.21	8.17	-	8.35	-	-	-	-0.18
G538	5	-0.32	-0.12	-	-0.18	8.11	-	8.37	-	-	-	-0.26
G458	1	-0.37	-0.17	0.80	-0.50	8.01	8.40	8.00	8.55	0.27	0.41	0.01
G266	1,6	-0.50	-0.47	1.53	-0.23	7.58	9.00	8.14	9.02	0.87	0.04	-0.56
G423	1,6	-0.51	0.07	0.94	-0.16	8.11	8.40	8.2	8.58	0.44	0.51	-0.09
G144	2	-0.31	-0.55	-	-	7.69	-	-	-	-	-	-
G231	2	-0.10	-0.46	-	-0.21	7.99	-	8.56	-	-	-	-0.57
G317	2	-0.24	-0.42	-	-	7.89	-	-	-	-	-	-
K supergiant												
NGC1948	7	-0.39	-0.21	0.39	-0.25	7.95	7.97	8.23	8.26	0.0	0.955	-0.11
Mean for F-G-K supergiants												
Mean (16 stars)	-	-0.30	-0.24	+0.91	-0.19	8.00	8.44	8.37	8.60	0.39	0.48	-0.32
std. dev.	-	± 0.11	± 0.18	± 0.47	± 0.11	± 0.19	± 0.43	± 0.17	± 0.31	± 0.36	± 0.37	± 0.20
Other objects :												
Sun	8	0.00	0.00	0.00	0.00	8.55	7.97	8.87	8.65	0.00	3.80	-0.32
Canopus	9	-0.07	-0.33	0.32	-0.16	8.15	8.22	8.64	8.56	-0.09	0.85	-0.49
Orion (B stars)	10	-0.03	-0.19	-0.17	-0.14	8.36	7.84	8.70	8.47	-0.15	3.31	-0.34
HII-SMC	11	-	-	-	-	-	-	8.09	-	-	9.38	-0.72
HII-SMC	12	-	-	-	-	7.16	6.46	8.02	7.24	-	5.01	-0.86
HII-LMC	12	-	-	-	-	7.90	6.97	8.43	7.95	-	8.51	-0.53
HII-Gal.	12	-	-	-	-	8.46	7.57	8.70	8.51	-	7.76	-0.24
SNR-SMC	13	-0.53	-	-0.56	-0.41	-	6.88	7.93	-	-	-	-
SNR-LMC	13	-0.28	-0.61	-0.24	-0.34	7.66	7.45	8.25	7.87	-0.50	1.62	-0.59

(a) the standard notation $\epsilon(\text{X}) = \log N(\text{X}) = \log [n(\text{X})/n(\text{H})] + 12$, where n = number density of atoms, is adopted; (b) Sources: (1) LL92, (2) RB89, (3) SBS89, (4) Rolleston et al. (1993), (5) Hill et al. (1995), (6) Barbuy et al. (1994), (7) Spite et al. (1993) (8) Grevesse & Noels (1993), (9) Luck & Lambert (1985), (10) Cunha & Lambert (1994), (11) Garnett et al. (1995), (12) Dufour (1984), (13) Russell & Dopita (1990).

5.1. Oxygen abundances

Before discussing the oxygen abundances in the Magellanic Clouds, it is worth recalling that oxygen is an element mostly produced in high mass Type II supernovae (SN II), while iron is thought to be most efficiently produced in Type Ia supernovae (SN I), exploding from longer-lived lower-mass binary progenitors. A mean underabundance of $[\text{O}/\text{Fe}] \approx -0.18 \pm 0.10$ dex relative to iron is found for our sample stars. In Fig. 6, we plot the oxygen-to-iron ratio against the iron abundance for the

SMC and the LMC supergiants (Hill et al. 1995). The location of Galactic supergiants (hatched area) and their mean value, with the abundance of the B stars in the Orion Nebulae are also indicated.

All the supergiants in our Galaxy and in the Magellanic Clouds are massive objects which have a very short life-time, and thus their atmospheres a representative of the young material of the galaxies, as the H II regions.

The most striking feature of Fig. 6 is the uniformly low $[\text{O}/\text{Fe}]$ ratio in the *young objects* of the three galaxies: an

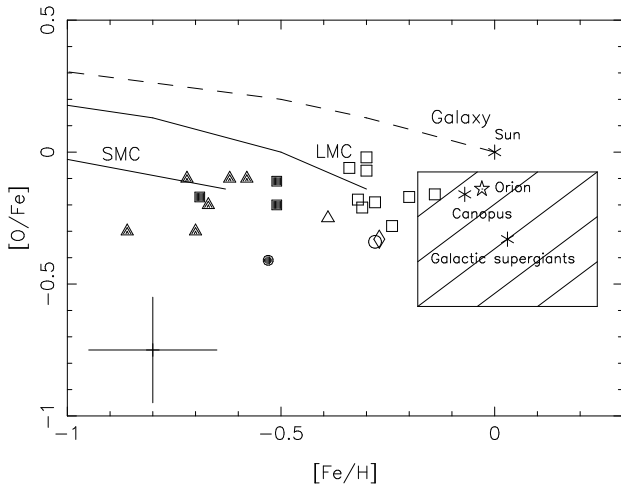


Fig. 6. $[O/Fe]$ versus $[Fe/H]$. For the Galaxy: Sun and Canopus (asterisks) and a mean for Orion B stars from Cunha & Lambert (1994) (open star), where the vertical line shows the r.m.s. For the SMC: K supergiants (filled triangles; this work), F supergiants (filled squares; SBS89). For the LMC: K supergiants (open triangles; Spite et al. 1993), F supergiants (open squares; Hill et al. 1995). The mean for SMC (filled circle) and LMC (open circles) SNR (Russell & Dopita 1990) and LMC type I planetary nebulae (Freitas Pacheco et al. 1993) (open diamond) are also displayed. The chemical evolution models by RD92 are shown for the Galaxy (dashed line), the LMC and the SMC (solid lines).

oxygen-to-iron overdeficiency of -0.3 to -0.2 dex is found in Galactic supergiants and ISM of the solar neighbourhood. Therefore, the present day -0.18 dex (SMC) and -0.15 dex (LMC) oxygen overdeficiencies are similar to what is observed in *similar objects* in the Galaxy. In this picture, there is no need for an IMF different in the Clouds and the Galaxy: the Magellanic Clouds could have had a continuous star formation, but with a lower rate (per unit gas mass), than in our Galaxy. This picture would also be compatible with a formation rate occurring in bursts: to discriminate between star formation occurring continuously or in bursts, the only probes lie in the past. At the time when the burst(s) occur, the $[O/Fe]$ must have changed very rapidly upon very small change of $[Fe/H]$ (Tsuji-moto et al. 1995): the observed $[O/Fe]$ should therefore be very dispersed for a given $[Fe/H]$ value (corresponding to the time of burst).

Since, magnesium, like oxygen, is believed to be produced in massive SN II, the $[Mg/Fe]$ ratio is expected to be about the same in the young objects of the SMC, the LMC and the Galaxy, as is indeed observed. Let us remark that in this picture, there is no need for a different IMF in the Clouds and the Galaxy.

The $[O/Fe]$ ratios measured in the SMC and LMC (see also Barbuy et al. 1994) are also in agreement with more complex scenarios of chemical evolution in the Clouds (Russell & Dopita 1992 hereafter RD92; Tsujimoto et al. 1995). This is not very surprising since these models were fitted to the $\epsilon(O)$ for the H II regions of each Cloud: it only reflects the good agreement between the stars and H II regions.

To achieve the low metallicity of the young material in the Clouds, the RD92 models assume that the formation of stars in the Clouds began later than in our own Galaxy (about 8 Gyrs ago instead of 15 Gyrs in our Galaxy). The young material in the Clouds should thus be similar to material as it was 7 Gyrs ago in our Galaxy. Since, it is well known that $[O/Fe]$ decreases with time (Edvardsson et al. 1993), we should expect a higher $[O/Fe]$ ratio in MC's young objects than in their Galactic counterparts. From Fig. 6, no difference is observed. To achieve the low observed $[O/Fe]$ ratio, the RD92 models used an IMF steeper in the Clouds than in the Galaxy (exponents of the power laws of respectively 1.8, 2.2, and 2.35 in the Galaxy, LMC and SMC).

However, other α -elements such as Mg, Si and Ca (which are also produced efficiently in massive SN II) do not show the same over-deficiency with respect to iron (Paper I; Hill et al. 1995), and these steep-IMF models would have problems to explain.

5.2. Convective mixing effects on C and N abundances

Convective mixing brings CNO-processed material to the outer atmospheric layers during stellar evolution along the red giant branch. Such process can be detected through carbon deficiencies accompanied by nitrogen enhancements (the effect on oxygen is negligible or less pronounced, since the ON-cycle occurs in deeper layers relative to the CN-process). We find a mean carbon to iron deficiency of $[C/Fe] = -0.30 \pm 0.07$ dex compatible with mixing effects expected in such stars. The nitrogen enhancement, however is mild ($[N/Fe] = 0.22 \pm 0.12$ dex). Low values of $^{12}C/^{13}C = 10-20$, determined for three sample stars confirm that convective mixing has occurred in these stars.

Our mean $\epsilon(C) = 7.54$ is lower than the mean value from high resolution work for 7 F supergiants and 3 B supergiants (cf. Table 3) of $\epsilon(C) = 7.7$ and the values found from low resolution spectra of $\epsilon(C) = 7.93$ for 3 stars by Thévenin & Jasniewicz (1992), and of $\epsilon(C) = 7.85$ for 40 K supergiants by Meliani et al. (1995). Therefore we find a value closer to the one by Dufour (1984) of $\epsilon(C) = 7.16$, although not quite as low. A comparison with the recent HST data by Garnett et al. (1995) shows that $\log(C/O)$ for our stars is systematically higher by around 0.3 dex (see Table 2 and 3). The question of the carbon abundance in the Small Cloud thus appears to be still open.

A more secure way to consider the carbon and nitrogen is through the C+N abundance, which is only marginally dependent on the C_2 feature and mostly determined by the fit of the reliable CN feature: an overestimation of the carbon abundance by 0.2 dex leads (by fitting the CN feature) to an underestimation of the nitrogen abundance by 0.25 dex, but the (C+N) abundance is then only overestimated by 0.04 dex; under such circumstances, the C/N ratio would be overestimated by a factor of 3.

Our results constitute the first high resolution CNO derivation of field (cool) K supergiants in the SMC. LL92 give both C and N abundances for only two supergiants (non-Cepheid) (AzV121 and AzV369) showing a mean value of $C/N = 0.65$.

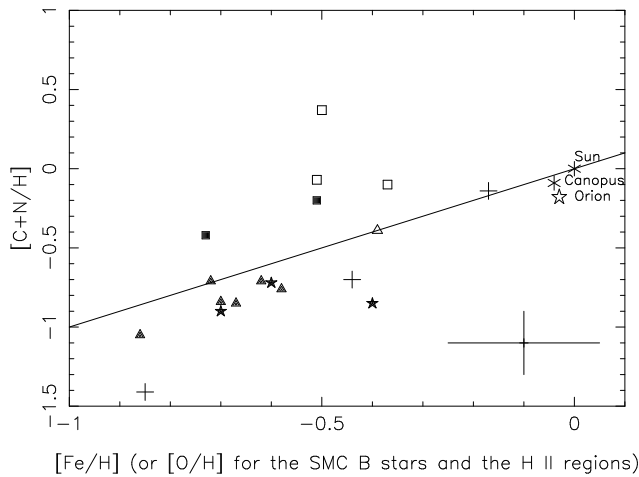


Fig. 7. $[(C+N)/H]$ versus $[Fe/H]$ (or versus $[O/H]$ for the H II regions and the B stars). For the SMC: K supergiants (filled triangles; this work), F supergiants (filled squares; LL92) and B stars (filled stars). For the LMC: K supergiants (open triangles; Spite et al. 1993), F supergiants (open squares; Hill et al. 1995, and open squares; RB89, LL92). The mean for SMC, LMC and the Galaxy H II regions (Dufour 1984) are also displayed (crosses). The solid line indicates $[(C+N)/Fe] = [Fe/H]$.

The mean value for our sample is $C/N = 1.27 \pm 0.28$, clearly below the solar value, but not as mixed as the two LL92 stars.

Our mean $[(C+N)/Fe] = -0.15 \pm 0.08$ dex, on the other hand, is close to the solar ratio, whereas for AzV121 and AzV369 there seems to be an excess of C+N ($[(C+N)/Fe] = 0.31$), arising from the very strong nitrogen abundance found by LL92 for these stars. Such a large difference is not easily understandable, even if the mixing is larger in these two stars. Since the lines used in the analysis are different, there could be a systematic effect in the derivations by LL92 and/or by us, and particularly for nitrogen.

In Fig. 7 we show $\epsilon(C+N)$ versus $[Fe/H]$, or versus $[O/H]$ for the H II regions and B stars, for the data reported in Tables 2 and 3. The solid line indicating $[(C+N)/Fe] = [Fe/H]$ represents approximately the behaviour of dwarf stars in our Galaxy. The C+N overdeficiency in the SMC is of the same order as that found in our Galaxy between the Sun and the solar neighbourhood young objects such as main sequence B stars in Orion and supergiants. The H II regions abundances in the Galaxy are consistent with that of these young objects, whereas the H II regions in both Clouds show a strong overdeficiency of C+N relative to supergiants. In fact, Garnett et al. (1995) have found that C/O in the H II regions of metal-poor dwarf irregular galaxies (including the SMC) are low; could this be an indication that the Clouds are indeed depleted in carbon, or maybe locked into grains?

5.3. Lithium

Lithium is detectable in all the program stars, and its abundance ranges from $\epsilon(Li) = 0.0$ to 0.6 dex. In fact, two of our stars

(PMMR 27 and PMMR 145) display a strong lithium abundance ($\epsilon(Li) = 0.6$ dex), while the four others show milder abundances ($\epsilon(Li) \approx 0.0$ dex). In other supergiant stars of the Magellanic Clouds, very few results are available; LL92 obtained only upper limits for lithium abundance owing to the faintness of the line in the hotter F supergiants. Previous determinations in Magellanic K supergiants only concern three stars: in the LMC NGC1948:WBT 542 and NGC1818:B12 and in the SMC NGC330 A7 (Spite et al 1993; Richtler et al. 1989; Spite et al. 1986). We have recomputed the lithium abundance in these stars using the present line list and the atmospheric parameters from the above papers, and we found values of respectively < 0.0 , 0.3 and 0.0. Smith and Lambert (1990) observed very strong lithium lines for Magellanic M stars in the AGB phase, and only in a limited range of luminosity. Therefore, for stars such as our supergiants which are not in the AGB phase, low lithium is expected.

Of course, the lithium that we observe is the original lithium abundance of the star, strongly diluted by convective mixing with the deep layers of the star, where the lithium has been destroyed. In our Galaxy, the massive ($\approx 9M_{\odot}$) K supergiants analysed by Luck (1977) show lithium abundances in the range -0.6 to $+1.0$ dex (mean value $\epsilon(Li) = 0.12$ dex) for all the stars with $T_{\text{eff}} \leq 4500$ K. If the initial Li abundance of these stars was the standard abundance of the young Pop I, the dilution would be -2.3 to -3.9 dex (including non-LTE corrections). The theoretical calculations for dilution of Li in the convective zone of massive stars have not made much progress in the recent years, and we must therefore recall Iben (1966) for an estimation of it. As advocated by Spite et al. 1986, this dilution and the possible non-LTE effects in the Li line brings the lithium abundance of the star up by $+1.8 \pm 0.3$ dex, leaving us with values of $\epsilon(Li)$ ranging from 1.8 to 2.4 dex for the stars in our sample. However, such a value is largely uncertain. If the dilution is similar to the dilution found in Luck's supergiants, the initial lithium abundance would be 2.9 to 3.9 dex.

6. Conclusions

The average oxygen deficiency of $[\overline{O/Fe}] = -0.18$ dex for the SMC supergiants is similar to what is found in the LMC (-0.15 dex) and for Galactic supergiants and other young objects (-0.2 to -0.3 dex). This result is of great importance in understanding the chemical evolution of the Magellanic Clouds, and could mean that the Clouds and the Galaxy have achieved the same level of chemical evolution, although the Clouds would have had a star formation rate (per unit gas mass) lower than in the galaxy. However, to constrain models, the oxygen abundance in older objects such as 12 Gyr globular clusters and intermediate age objects (≈ 4 Gyr) are badly needed, in particular, to discriminate between star formation occurring in bursts or continuously.

Carbon deficiencies ($[\overline{C/Fe}] = -0.3$ dex) and nitrogen enhancements ($[\overline{N/Fe}] = +0.22$ dex), together with the low $^{12}C/^{13}C$ of 10-20 are indicative of a mild convective mixing.

Lithium abundances are found within the range $\epsilon(\text{Li})=0.0$ to 0.6 dex, which are compatible with the values found for similar stars in the Galaxy, thus indicating that mixing has occurred in the Magellanic K supergiants, in agreement with the measured $^{12}\text{C}/^{13}\text{C}$ and C/N ratios.

Carbon plus nitrogen ($[\text{C}+\text{N}/\text{Fe}]$) abundances are mildly deficient in our sample of K supergiants, whereas it appears overabundant in F supergiants in the SMC and the LMC. Since the lines used are different, there could be systematic effects in the abundance determinations. In the H II regions, it appears even more drastically deficient than in our K supergiants. In order to resolve this puzzle, it would be important to analyse larger samples of F, G, K supergiants, and to have a better understanding of the HII regions.

References

- Barbuy, B., 1981, A&A, 101, 365
 Barbuy, B., 1988, A&A, 191, 121
 Barbuy, B., Freitas Pacheco, J.A., Castro, S., 1994, A&A, 283, 32
 Cayrel, R., Perrin, M.-N., Barbuy, B., Buser, R., 1991, A&A, 247, 108
 Cunha, K., Lambert, D.L., 1994, ApJ, 426, 170
 Dufour, R.J., 1984 in: *Structure and evolution of the Magellanic Clouds* IAU Symp. 108, eds. S. Van den Bergh, K. de Boers, Reidel, Dordrecht, p.353
 Dufour, R.J., Shields, G.A., Talbot, R.J., 1982, ApJ 252, 461
 Edvardsson, B., Andersen, J., Gustafsson, B., Lambert D.L., Nissen, P.E., Tomkin, J., 1993, A&A 275, 101
 de Freitas Pacheco, J.A., Barbuy, B., Costa, R.D.D., Idiart, T.E.P., 1993, A&A, 271, 429
 Garnett, D.R., Skillman, E.D., Dufour, R.J., Peimbert, M., Torres-Peimbert, S., Terlevich, R., Terlevich, E., Shields, G.A., 1995, ApJ, 443, 64
 Grevesse, N., Noels, A., Sauval, J., 1996, in ASP Conf. Series 99, S.S. Holt, G. Sonneborn eds, p. 117
 Hill, V., Andrievsky, S., Spite, M., 1995, A&A, 293, 347
 Hill, V., 1996, A&A in press (Paper I)
 Iben, I.Jr., 1966, ApJ 143, 483
 Kraft, R. P., 1994, PASP 106, 553
 Lambert, D.L., Smith V., Heath, J., 1993, PASP, 105, 568
 Lambert, D.L., Sneden, C., Ries, L.M., 1974, ApJ, 188, 97
 Luck, R.E., 1977, ApJ 218, 752
 Luck, R.E., Lambert, D.L., 1985, ApJ, 298, 782
 Luck, R.E., Lambert, D.L., 1992, ApJS, 79, 303 (LL92)
 Meliani, M., Barbuy, B., Richtler, T., 1995, A&A, in press
 Milone, A., Barbuy, B., Spite, M., Spite, F., 1992, A&A, 261, 551
 Plez, B., Brett, J.M., Nordlund, A., 1992, A&A, 256, 551
 Prévot, L., Martin, N., Maurice, E., Rebeiro, E., Rousseau, J., 1983, A&AS, 53, 255 (PMMR)
 Richtler, T., Spite, M., Spite, F., 1989, A&A 225, 351
 Rocca-Volmerange, B., Prévot, L., Ferlet, R., Lequeux, J., Prévot-Burnichon, M.L., 1981, A&A, 99, L5
 Rolleston, W.R.J., Dufton, P.L., Fitzsimmons, A., Howarth, I.D., Irwin, M.J., 1993, A&A 277, 10
 Russell, S.C., Bessell, M.S., 1989, ApJS, 70, 865 (RB89)
 Russell, S.C., Dopita, M.A., 1990, ApJS, 74, 93
 Russell, S.C., Dopita, M.A., 1992, ApJ, 384, 508 (RD92)
 Smith, V.V., Lambert, D.L., 1990, ApJ 361, L69
 Spite, M., Barbuy, B., Spite, F., 1989a, A&A, 222, 35 (SBS89)
 Spite, F., Barbuy, B., Spite, M., 1993, A&A, 272, 116
 Spite, M., Cayrel, R., François, P., Richtler, T., Spite, F., 1986, A&A 168, 197
 Spite, F., Spite, M., François, P., 1989b, A&A, 210, 25
 Spite, M., 1967, Ann. d'Astrophys., 30, 211
 Spite, M., 1990, 2nd ESO/ST-ECF Data Analysis Workshop, ESO Conf. and Workshop Proc. 34, eds. D. Baade & P.J. Grösbol, p. 125
 Thévenin, F., Jasniewicz, G., 1992, A&A, 266, 85
 Tsujimoto, T., Nomoto, K., Yoshii, Y., Hashimoto, M., Yanagida, S., Thielemann, F.-K., 1995, MNRAS 277, 945